Control of a Snake Robot for Ascending and Descending Steps

Motoyasu Tanaka and Kazuo Tanaka

Abstract—This paper proposes control method for a snake robot to ascend and descend steps. In a multi-plane step environment, it is necessary for locomotion to transfer from one plane to another. When a snake robot moves, it touches several planes as its body is long and thin. In this paper, we propose a control method to track the trajectory of a snake robot in a step environment. We decomposed the three-dimensional motion of the robot into two simple models by introducing an assumption that simplifies the model and controller, and derive a model of the robot as a hybrid system with switching. The control method consists of a tracking controller, a method for shifting the robot's part connecting the planes, and active lifting to control the shape of the robot. Ascent and descent experiments confirm the effectiveness of the proposed controller and the method for shifting the connecting part of the robot's body.

Index Terms—Snake robot, Step climbing, Switching constraints, Redundancy, Kinematics.

I. INTRODUCTION

Snakes can locomote in various environments, e.g., on uneven terrain, along walls, underwater, and in trees, despite their simple limbless bodies. Snake robots are expected to be able to locomote in similar environments. However, it is difficult to control a snake robot owing to the large number of actuators and because it moves by utilizing the friction force of its body. This paper deals with a snake robot that moves by using the friction of its body and a bending motion without generating propulsion through active wheels or crawlers.

Hirose has been developing the snake robot [1] as an "active cord mechanism" since 1972. The robot locomotes by "shift control" where the bending motion of the frontal segment shifts to rear segments. The computational cost of the method is small and the method is suitable for a snake robot, which is a resource limited system because of its thin body. The method has been used not only in snake robots, but also in articulated mobile robots [2]–[5], which have a mechanism to generate propulsion directly. Recently, there has been an increase in the number of studies of a snake robot focusing on intended three-dimensional rather than two-dimensional motion. A backbone curve [6], representing the curve of the body of a snake robot, has typically been used to generate three-dimensional motion. The backbone curve and its extension were proposed for multiple three-dimensional gaits, e.g., sidewinding, pole climbing, and helical rolling [7]–[10]. In these methods, the body shape is defined using a continuous curve or joint angles, and the robot moves using a shift of the body shape as shift control. However, no mathematical proofs for tracking the desired trajectory have been provided for any of these methods.

Tracking controllers of a snake robot for a two-dimensional plane were proposed in [11]–[19]. Two modeling methods are mainly used to implement tracking controllers for snake robots. The first method considers anisotropic friction of the robot's body [11], [12]. Liljebäck et al. proposed a straight line path-following controller for the center of gravity [11], [12]. The model used in the controller is based on the dynamics considering anisotropic ground friction. However, this model is more complex than that based on another method described below and the robot's head cannot track the desired trajectory in [11], [12].

The other method considers velocity constraints, which prevents the body from slipping sideways [13]–[19]. Prautsch et al. accomplished stabilization of the position of a snake robot using Lyapunov's method, but the robot converged to a singular configuration, e.g., a straight line or an arc [13]. Methods for singularity avoidance of a snake robot were proposed by [14]–[18]. Date et al. avoided singularity by considering dynamic manipulability [14], while Yamakita et al. did so by reducing the constraint force in a head-raising snake robot [15]. Dynamic modeling was used to consider the dynamic properties in the controller design, but there is a trade-off between singularity avoidance and convergence of the tracking error in [13]–[15]. Snake robots can effectively search narrow spaces and are remotely controlled using sensors on the robot. Trajectory tracking of the head is important because the operator generally controls the articulated robot by indicating the desired direction of the head [20], [21], [26]. Matsuno found that the introduction of links without wheels turned the robot into a kinematically redundant system. He proposed a controller that accomplishes both trajectory tracking of the robot's head and subtasks like singularity avoidance using redundancy based on kinematic [16] and dynamic [17] models, and with other subtasks for a head-raising snake robot [18].

In the case of three-dimensional motion on a plane, the main problem is determining which parts of the body of the snake robot should be grounded and which should be raised. We proposed a model and controller considering the switching of grounding parts and obtained tracking motion with moving obstacle avoidance [19]. With respect to control in a smooth three-dimensional environment, trajectory tracking control on a cylindrical surface has been proposed [22]. However, there have been no reports of tracking of the desired trajectory to control snake robots in three-dimensional discrete environments like steps and stairs.

Many articulated mobile robots with a similar shape to the snake robot, have been developed [2]–[5], [20], [23]–[27]. These robots have several segments serially connected by joints, and each segment has a mechanism to generate propulsion directly, e.g., active wheels and tracks. For articulated mobile robots, there are two well-known control methods, "follow-the-leader" and "n-trailer." "Follow-the-leader", used in [2]–[5], [24]–[27], is a method in which the robot is controlled by having all segments repeat the motion pattern of the first segment. This method is similar to shift control in snake robots. The motion of following segments is defined by shift control in [2]–[5], using inverse kinematics as all the segments follow the path of the first segment in [24], and by approximate discretization of a continuous curve in [25]–[27]. The "n-trailer" control method used in [20], [28], is a method in which the motion of the whole body is treated as a active track pulling n passive trailers connected behind it. The following segments move in a passive manner based on a kinematic model. This method is similar to the tracking controllers of the snake robots in [13]–[19] because the model used in the method is derived using the same assumption, which means that the wheels do not slip laterally. In three-dimensional environments, KR-I [2] climbed stairs, an articulated robot for sewer inspection [24] climbed from a horizontal plane to a horizontal pipe, ACM-R4 [25] climbed onto a chair, and ACM-R4.1 [26] and R4.2 [27] adaptively moved forward on uneven terrain by shift control with compliance control using torque sensors. These robots do not need to undulate laterally because the propulsion is generated by active wheels and tracks. Thus, since a snake robot must undulate laterally to obtain propulsion force, the methods for articulated mobile robots cannot be applied to it. In a snake robot, cooperative motion between the horizontal and vertical

M. Tanaka and K. Tanaka are with the Department of Mechanical Engineering and Intelligent Systems, The University of Electro-Communications, Tokyo 182-8585 Japan. (e-mail: mtanaka@uec.ac.jp).

Fig. 1. An n-module snake robot.

(a) Descending case   (b) Ascending case

Fig. 2. Step environment and a snake robot.

Fig. 3. Ascending phase of the snake robot. The snake robot (a) locomotes on the rear plane, (b) raises its head when approaching the front plane, (c) locomotes while shifting between the two planes, and (d) locomotes on the front plane.
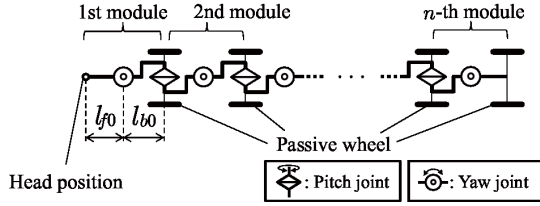
motions is needed in a three-dimensional environment.

This paper proposes a control method to accomplish trajectory tracking of the robot's head and moving up and down in a step environment consisting of two horizontal planes. We model the snake as a two-dimensional snake robot in which the grounding condition of the wheels switches dynamically and the length of the projection of links changes on a plane, by devising the motion of the "connecting part," which is the part of the robot's body connecting the two planes. We propose a controller based on kinematics to accomplish trajectory tracking considering the condition of the robot straddling two planes, and a shifting method for the part of the robot connecting the planes to accomplish moving from the front plane to the rear plane. The proposed shifting condition prevents collisions between the robot and the step during descent. Experiments show the effectiveness of the proposed control method. The proposed controller comprises a framework for a tracking controller incorporating shift control as a component. The joint reference for horizontal motion to ascend and descend a step is generated as shift control using the follow-the-leader method for articulated mobile robots, while the lateral motion on the upper and lower planes is calculated considering horizontal motion as traditional tracking controllers.

Our goal is to achieve autonomous control of a snake robot for search and rescue operations arising from some disaster in a rubble-strewn habitation environment, e.g., a collapsed building and underground mall. The habitation area is an artificial environment containing planes, e.g., walls and floors, and smooth curved surfaces, e.g., pipes. Locomotion is possible in the area in that the robot can locate "available areas" for traction and to generate a propulsion force and can move through the areas avoiding obstacles. However, if the available areas are not adjacent, the robot has a problem moving from one to the next. In this paper, we focus on two parallel planes, which is one of the simplest configurations of pairs of available areas and derive a model and design the controller to implement a shift of the robot from one plane to the other. Although two parallel planes is a simple configuration, the controller can be applied to the motion of stair climbing, which is a more difficult field to maneuver through in a habitation area. Here, we apply the proposed controller to climbing stairs, while dealing with other pairs of surfaces, e.g., non-parallel planes or a plane and curved surface, is left for future work. The effect of gravity on the locomoting robot is not large in this study and the robot can locomote using the proposed controller based on kinematics since the assumed environment consists of two horizontal planes. However, it would be necessary to consider a dynamic analysis in the case of two nonparallel planes because the effect of gravity would play a major role in this case. Considering these dynamics is left as a future work.

II. MODELING

We consider an n-module snake robot as shown in Fig. 1. The module of this robot has a yaw rotational joint and is connected in series via a pitch rotational joint. The passive wheel is coaxially placed with the pitch joint and velocity constraint, preventing side slip
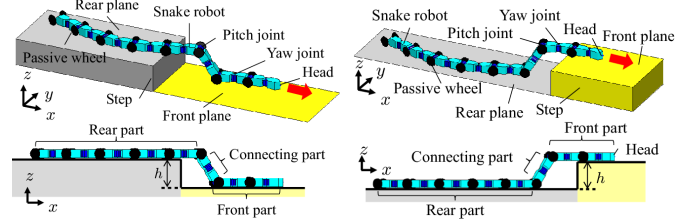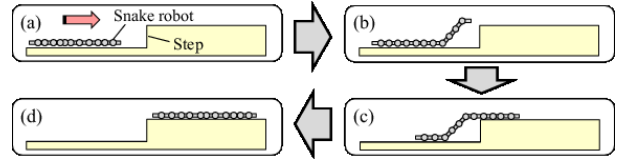
from occurring if the wheel touches the ground. The snake robot can perform the same locomotion as a living snake by bending its joints appropriately considering the velocity constraint. l_{f0} is the length from the anterior end of the link to the axis of the yaw joint, l_{b0} is the length from the posterior end of the link to the axis of the yaw joint, and $L = l_{f0} + l_{b0}$. Let ϕ_i be the yaw joint angle of the i-th module, ψ_i be the pitch joint angle between the i-th and $i+1$-th module, and let us define $\boldsymbol{\psi} = [\psi_1, \cdots, \psi_{n-1}]^T$, and $\boldsymbol{\phi} = [\phi_1, \cdots, \phi_n]^T$.

A. Step environment

Fig. 2 shows the step environment and the snake robot discussed in this paper. The environment consists of a step of height h against the xz-plane in the absolute coordinate system Σ_{xyz} in the step environment, which is spatially uniform to the y-axis. The robot moves down the step if $h < 0$, and up the step if $h > 0$. In the case where the snake robot moves in a step environment consisting of a number of planes, it is necessary for the robot to generate propulsion force by touching its wheels on each plane. The snake robot can locomote in this environment by moving both the parts touching the planes and those connecting the planes, although this is difficult to control as the model is a hybrid system involving dynamic switching of the touch conditions between the wheels and planes.

We can break down the ascending and descending motion on a step into four phases. Fig. 3 shows the ascending phase of the snake robot. Realizing the movement in (a) and (d) can be accomplished by the methods in [11]–[14], [16], [17], while that in (b) can be accomplished by the method proposed in [15], [18]. Thus, this paper focuses on locomotion while shifting between two planes as shown in (c).

Regarding the robot, we call the part whose wheel touches the front plane of the step environment the "front part," that whose wheel touches the rear plane the "rear part," and that between the front part and the rear part the "connecting part," as shown in Fig. 2. It is preferable for the connecting part to be shifted back and forth depending on the motion. For example, we consider locomotion in the direction of the x-axis from the state shown in Fig. 2(a) with the
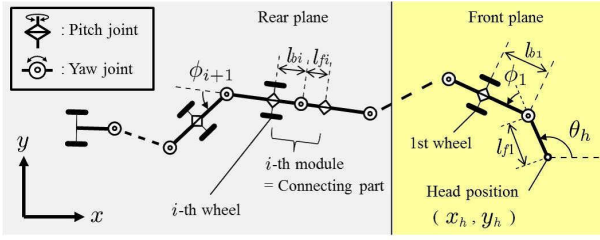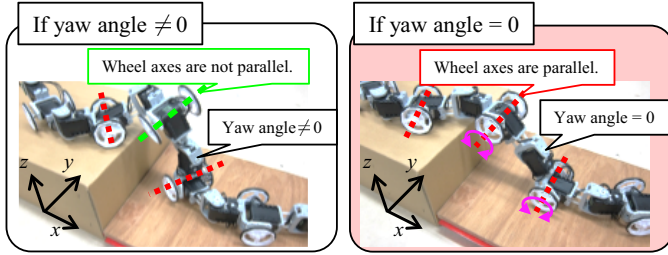
Fig. 4. xy-projection model of the snake robot.

Fig. 5. The yaw angle of the connecting part and wheel axes.

connecting part fixed. The load on the pitch joints increases with an increasing number of ungrounded wheels corresponding to an increase in the distance of locomotion. As more wheels touch the ground and the load on the joints decreases, it is necessary to shift the connecting part in the posterior direction. In the case where the robot climbs a step, as shown in Fig. 2(b), if the robot does not shift the connecting part, it collides with the step. Thus, the snake robot needs to shift its connecting part to climb and descend a step.

Complicated motion is needed to plan the joint angle of the connecting part and to shift it with the wheels touching each plane. Thus, the following assumption is introduced.

[Assumption 1]: The yaw angle of the connecting part is zero.

By assumption 1, the direction of the wheel axis of the connecting part is the same as those of the anterior and posterior wheels as shown in Fig. 5, and the connecting part can connect the front and rear parts such that each wheel touches each plane. In this case, planning of the connecting part only requires appropriately controlling the angles of the pitch joints.

By introducing this assumption, the shift in the connecting part can be planned based only on the pitch joint angles. Therefore, it is possible to deal with three-dimensional motion by breaking it down into motion parallel to the xy-plane and that parallel to the z-axis. In this paper, we consider the case where the connecting part consists of one module and $|h| < l_{f0} + l_{b0}$. However, the model and controller presented in this paper can be applied to higher steps by increasing the number of links in the connecting part.

B. Kinematic model

The robot can be treated as a two-dimensional snake robot by projection onto the xy-plane as shown in Fig. 4. Note that ungrounded wheels are not shown in Fig. 4 (e.g., the $i-1$-th wheel). On the xy-plane, let $w = [x_h, y_h, \theta_h]^T$ be the position and attitude of the robot's head and ψ_h be the absolute pitch attitude of the robot's head, and let us define $\Psi_i = \psi_h + \Sigma_{j=1}^{i-1}\psi_j$ and $|\Psi_i| \le \frac{\pi}{2}$. l_{fi} and l_{bi} are the projections of l_{f0} and l_{b0} on the xy-plane, respectively. Note that l_{fi} and l_{bi} change with the pitch joint angle because they are projections on the xy-plane and the state of whether each wheel touches the ground is switched dynamically by the position and body

shape of the robot. l_{fi} and l_{bi} are expressed as

$$l_{fi} = l_{f0}\cos\Psi_i, \quad l_{bi} = l_{b0}\cos\Psi_i. \tag{1}$$

We set $l_f = [l_{f1}, \cdots, l_{fn}]^T$, $l_b = [l_{b1}, \cdots, l_{bn}]^T$, and $l_{all} = [l_f^T, l_b^T]^T$. On the xy-plane, the velocity constraints preventing side slip if all wheels are touching the ground as in [16], [17], are expressed as

$$A\dot{w} = [B_\phi \quad B_l]\begin{bmatrix} \dot{\phi} \\ \dot{l}_{all} \end{bmatrix}, \tag{2}$$

where $A \in \mathbf{R}^{n\times3}$, $B_\phi \in \mathbf{R}^{n\times n}$, and $B_l \in \mathbf{R}^{n\times2n}$.

We set $\psi_h = \dot{\psi}_h = 0$ because the robot's head continues to move on the same plane during locomotion while shifting between two planes as shown in Fig. 3(c), and the derivation of (1) is given by

$$\dot{l}_{all} = B_\psi\dot{\psi}, \tag{3}$$

where $B_\psi \in \mathbf{R}^{2n\times(n-1)}$. By substituting (3) into (2), we obtain

$$A\dot{w} = Bu, \tag{4}$$
$$B = [B_\phi \ B_l]\begin{bmatrix} I_n & 0 \\ 0 & B_\psi \end{bmatrix} = [B_\phi \ B_lB_\psi], \ u = \begin{bmatrix} \dot{\phi} \\ \dot{\psi} \end{bmatrix},$$

where $I_j \in \mathbf{R}^{j\times j}$ is the identity matrix. Each row of the matrices in (4) represents the velocity constraint of the corresponding wheel preventing side slip, e.g., the i-th row represents the velocity constraint of the i-th wheel. The kinematic model of the snake robot on the xy-plane changes depending on both the state of whether each wheel is touching the ground and that of the connecting part. We consider the case where the wheels of n_σ modules ($j_1, \cdots, j_{n_\sigma}$-th) are ungrounded and with n_c modules ($k_1, \cdots, k_{n_c}$) in the connecting part. We refer to the unique integers derived from both the state of allocation of wheeled links and that of the connecting part as "modes" and denote the discrete mode number as σ. When the mode of the robot is σ, the velocity constraints are expressed as

$$\bar{A}_\sigma\dot{w} = \bar{B}_\sigma u, \tag{5}$$

where $\bar{A}_\sigma \in \mathbf{R}^{(n-n_\sigma)\times3}$ and $\bar{B}_\sigma \in \mathbf{R}^{(n-n_\sigma)\times(2n-1)}$ are the matrices, excepted $j_1, \cdots, j_{n_\sigma}$-th rows from A and B, respectively. For two-dimensional snake robots, the joint angle corresponding to an ungrounded wheel is included in the controlled variables as the "shape controllable point" (SCP) [16], [17]. There is a distinct connecting part for ascending and descending a step in this paper, and it is necessary to include the yaw angles of the connecting part in the controlled variables to satisfy assumption 1. Then, we introduce the following two elements into the controlled variables.

1) The yaw angles of the connecting part $\phi_c \in \mathbf{R}^{n_c}$.
2) The SCPs on the xy-plane ϕ_{scp} ([16], [17]), considering the case where the yaw angles of the connecting part are fixed as $\phi_c = 0$.

Now, the robot can move on the xy-plane using the traditional method and can directly control the yaw angle of the connecting part so as to satisfy assumption 1. We set $\theta = [\theta_h, \phi^T]^T$, $\tilde{\phi}_\sigma = [\phi_{scp}^T, \phi_c^T]^T \in \mathbf{R}^{n_\sigma}$, $\bar{w}_\sigma = [w^T, \psi^T, \tilde{\phi}_\sigma^T]^T$, and B', the selection matrix whose elements are 0 and 1, satisfying $B'u = \tilde{\phi}_\sigma$. By combining (5) and $B'u = \tilde{\phi}_\sigma$, the kinematic equation of the robot in mode σ on the xy-plane is expressed as

$$\tilde{A}_\sigma(\theta,\psi)\dot{\bar{w}}_\sigma = \tilde{B}_\sigma(\theta,\psi)u, \tag{6}$$
$$\tilde{A}_\sigma = \begin{bmatrix} \bar{A}_\sigma & 0 & 0 \\ 0 & I_{n-1} & 0 \\ 0 & 0 & I_{n_\sigma} \end{bmatrix}, \ \tilde{B}_\sigma = \begin{bmatrix} \bar{B}_\sigma \\ 0 \ I_{n-1} \\ B' \end{bmatrix},$$

where $\tilde{A}_\sigma \in \mathbf{R}^{(2n-1)\times(n+n_\sigma+2)}$ and $\tilde{B}_\sigma \in \mathbf{R}^{(2n-1)\times(2n-1)}$. Note that the matrices and vectors in (6) switch with mode σ. If we design
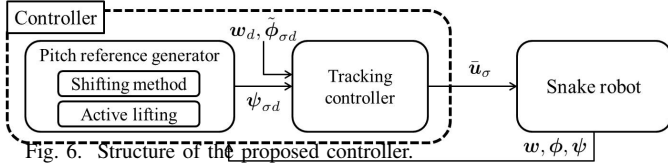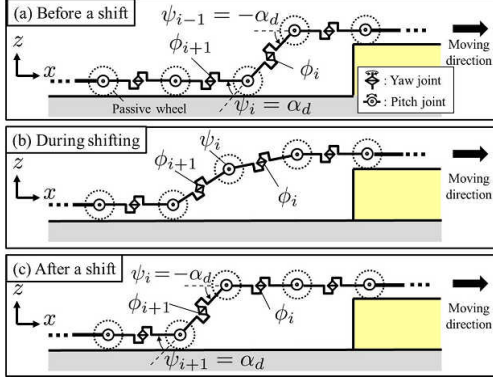
Fig. 6. Structure of the proposed controller.

Fig. 7. Shift of the connecting part.

the absolute angle of the SCPs instead of the relative angle thereof, we need to replace the corresponding element of $\tilde{\boldsymbol{\phi}}_\sigma$ with the absolute angle and to modify the corresponding row of $\boldsymbol{B}'$ accordingly. We design the controller of the robot's motion on the xy-plane using the kinematic model (6).

III. CONTROLLER DESIGN

The control input related to locomotion in the direction of the xy-axis is determined based on the kinematic model (6). Moreover, the connecting part is shifted in the posterior direction by determining the desired value of the pitch joints so that the ungrounded module sequentially touches the ground in the descending case and the grounded module is sequentially lifted up in the ascending case.

The motion of the robot is determined by the motion of the yaw and pitch angles, with a vector consisting of the angular velocity of the yaw and pitch joints used as the control input. The robot is propelled via serpentine motion using the yaw angle to move forward and the pitch angle to shift back the connecting part. The pitch angle is also used to raise certain wheels (referred to as active lifting). We also propose a controller, consisting of a pitch reference generator, which sets the pitch angle, and the tracking controller, which controls the input to the robot. Fig. 6 shows the structure of the proposed controller. The pitch reference generator determines the desired value of the pitch joint angles based on the shifting method and active lifting, and the tracking controller calculates the input velocity by which the controlled variable converges to the desired value.

A. Tracking controller

We set the desired vector of the controlled variable $\bar{\boldsymbol{w}}_\sigma$ as $\bar{\boldsymbol{w}}_{\sigma d} = [\boldsymbol{w}_d^T, \boldsymbol{\psi}_d^T, \tilde{\boldsymbol{\phi}}_{\sigma d}^T]^T$ where $\boldsymbol{w}_d = [x_{hd}, y_{hd}, \theta_{hd}]^T$ is the desired vector of the position and attitude of the robot's head. Let us define the control input $\boldsymbol{u}$ as

$$\boldsymbol{u} = \tilde{\boldsymbol{B}}_\sigma^{-1} \tilde{\boldsymbol{A}}_\sigma \left\{ \dot{\bar{\boldsymbol{w}}}_{\sigma d} - \boldsymbol{K}_\sigma \left(\bar{\boldsymbol{w}}_\sigma - \bar{\boldsymbol{w}}_{\sigma d} \right) \right\}, \tag{7}$$

where $\boldsymbol{K}_\sigma$ is the block diagonal matrix $\boldsymbol{K}_\sigma = \mathrm{diag}\,(\boldsymbol{K}_w,\ \boldsymbol{K}_\psi,\ \boldsymbol{K}_{\tilde{\phi}_\sigma})$, $\boldsymbol{K}_w \in \mathbf{R}^3$, $\boldsymbol{K}_\psi \in \mathbf{R}^{n-1}$, and $\boldsymbol{K}_{\tilde{\phi}_\sigma} \in \mathbf{R}^{n_\sigma}$ are the positive diagonal matrix. The matrix $\tilde{\boldsymbol{B}}_\sigma$ is invertible for all σ (the proof is

omitted for space limitations). The closed-loop system is expressed as

$$\tilde{\boldsymbol{A}}_\sigma \left\{ \left(\dot{\bar{\boldsymbol{w}}}_\sigma - \dot{\bar{\boldsymbol{w}}}_{\sigma d} \right) + \boldsymbol{K}_\sigma \left(\bar{\boldsymbol{w}}_\sigma - \bar{\boldsymbol{w}}_{\sigma d} \right) \right\} = \boldsymbol{0}. \tag{8}$$

If matrix $\tilde{\boldsymbol{A}}_\sigma$ is full column rank, the uniqueness of the solution is guaranteed. The solution of (8) is given as

$$\left(\dot{\bar{\boldsymbol{w}}}_\sigma - \dot{\bar{\boldsymbol{w}}}_{\sigma d} \right) + \boldsymbol{K}_\sigma \left(\bar{\boldsymbol{w}}_\sigma - \bar{\boldsymbol{w}}_{\sigma d} \right) = \boldsymbol{0}, \tag{9}$$

and $\bar{\boldsymbol{w}}_\sigma$ converges to the desired trajectory $\bar{\boldsymbol{w}}_{\sigma d}$ at $t \to \infty$ without switching the mode. If the robot has a singular configuration in which all wheels are parallel or arc-like, matrix $\tilde{\boldsymbol{A}}_\sigma$ is not full column rank. In this paper, θ_{hd} is set as a sinusoidal wave to avoid singular configurations [17]. In addition, it is important that $\tilde{\boldsymbol{A}}_\sigma$ is not a horizontally long matrix to obtain full column rank, and the following condition should be satisfied:

$$2n - 1 \geq n + n_\sigma + 2,$$
$$\therefore\ n_\sigma \leq n - 3. \tag{10}$$

Condition (10) means that there is an upper limit on the number of ungrounded modules and emphasizes the need for the ungrounded modules to touch the ground sequentially in the descending case.

Equation (9) has a feature that the controlled variable is switched depending on the mode. $\boldsymbol{w}$ and $\boldsymbol{\psi}$, which are involved in all modes, converge to the desired value because all the closed-loop systems corresponding to $\boldsymbol{w}$ and $\boldsymbol{\psi}$ are equally independent of the mode as given below.

$$(\dot{\boldsymbol{w}} - \dot{\boldsymbol{w}}_d) + \boldsymbol{K}_w(\boldsymbol{w} - \boldsymbol{w}_d) = \boldsymbol{0}, \tag{11}$$
$$(\dot{\boldsymbol{\psi}} - \dot{\boldsymbol{\psi}}_d) + \boldsymbol{K}_\psi(\boldsymbol{\psi} - \boldsymbol{\psi}_d) = \boldsymbol{0}. \tag{12}$$

However, in the case of arbitrary switching, the convergence of SCP $\tilde{\boldsymbol{\phi}}_\sigma$ is not ensured because the elements of the SCP are varied by switching the mode as follows.

$$(\dot{\tilde{\boldsymbol{\phi}}}_\sigma - \dot{\tilde{\boldsymbol{\phi}}}_{\sigma d}) + \boldsymbol{K}_{\tilde{\phi}_\sigma}(\tilde{\boldsymbol{\phi}}_\sigma - \tilde{\boldsymbol{\phi}}_{\sigma d}) = \boldsymbol{0}. \tag{13}$$

If the dwell time of each mode is sufficiently large, it is expected that $\tilde{\boldsymbol{\phi}}_\sigma$ converges adequately in each mode [29] [30]. The dwell time of each mode is described in a later section.

The desired values of SCP $\tilde{\boldsymbol{\phi}}_\sigma$ and pitch angle $\boldsymbol{\psi}$ are discussed in the next subsection to utilize the shift of the connecting part.

B. Pitch reference generator

Assume that the connecting part is the i-th module. The pitch reference generator, which is designed to shift the connecting part, consists of the shifting method and active lifting. The shifting method determines the reference to shift the connecting part from forwards to backwards depending on the motion, while the active lifting determines the reference to change the shape of the body of the robot and to prepare for the shift.

In this paper, we assume the connecting part is shifted as shown in Fig. 7. This figure depicts the robot (a) before the shift, (b) during the shift, and (c) after the shift of the connecting part in the ascending case, and is described for the case in which all yaw angles are zero for readability.

C. Active lifting for the additional SCP

We consider lifting up arbitrary wheels actively as shown in Fig. 8. If one wheel is lifted up, the corresponding velocity constraint disappears. The number of SCPs increases as the number of velocity constraints decreases [16]. These additional SCPs can affect the shape of the robot through direct control. If the lifting height is small, the lifting angle of the pitch joint does not affect the motion of the yaw
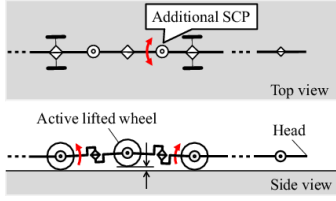
Fig. 8. Active lifting of the wheel.

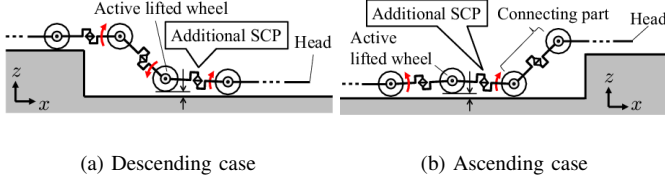(a) Descending case   (b) Ascending case

Fig. 9. Active lifting to descend and ascend a step.

angles. For descending, in our motion design the robot lifts up the wheel of the connecting part as shown in Fig. 9(a) and controls the absolute angle of the additional SCP. Fig. 9(b) shows the additional SCP in the ascending case. For ascending, the additional SCP is used as preparation for shifting as described in the next subsection.

D. Shifting method

In the shifting method, the reference of pitch joints is generated by transiting two states: (S1) preparation for shifting, and (S2) shift of the connecting part, as shown in Fig. 10.

1) Preparation for shifting: The yaw angle ϕ_{i+1} becomes the connecting part at the next shift because the i-th module is the connecting part. From assumption 1, it is necessary for ϕ_{i+1} to converge to zero before shifting the connecting part. In the descending case, the i-th wheel becomes ungrounded and ϕ_{i+1} becomes one of the SCPs by forward motion of the robot. In the ascending case, ϕ_{i+1} becomes an additional SCP by active lifting. As the SCP can be controlled directly, we set the desired value of ϕ_{i+1} to $\phi_{(i+1)d} = 0$, in preparation of shifting.

2) Shifting condition: If the robot satisfies the shifting condition, the state of the robot transits from (S1) to (S2). Let the border of the step be on the line $x = x_{step}$ and the direction of motion be the positive direction of x. In the descending case, let us define the shifting condition of the connecting part as follows:

$$|\phi_{i+1}| < \epsilon, \tag{14}$$
$$x_h - (i+1)L > x_{step}, \tag{15}$$

where $\epsilon > 0$ is a small value. ϕ_{i+1} is the yaw angle of the part that becomes the connecting part at the next shift. Condition (14) means that ϕ_{i+1} converges almost to zero and completion of the preparation for shifting is approximately satisfied if the condition is satisfied. The left-hand side of (15) denotes the minimum position of the x-axis of the $i + 1$-th module, which will become the connecting part at the next shift. Therefore, condition (15) guarantees that the wheel of the connecting part does not touch the step. This is a conservative condition to prevent the robot from colliding with the step, as shown in Fig. 11. It would appear that shifting the connecting part can be achieved by introducing (14) and (15) without colliding with the step.

In the ascending case, we set the following condition instead of (15).
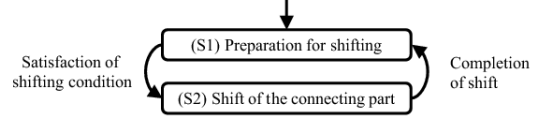
$$n_{nw} < a_{nw}, \tag{16}$$

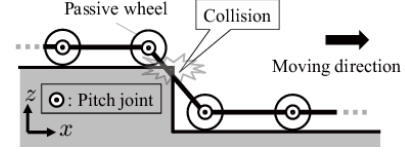Fig. 10. State transition of the shifting method.

Fig. 11. Collision with the step.

where n_{nw} is the number of ungrounded wheels in the front part and a_{nw} is an arbitrary integer satisfying $0 < a_{nw} \leq a_L$. Fig. 7(a) and (c) shows the cases for $n_{nw} = 1$ and $n_{nw} = 2$, respectively. a_L is the upper limit of a_{nw} depending on the maximum torque needed to hold up ungrounded wheels, and is calculated using statics. For example, if $a_{nw} = 2$, the robot in Fig. 7(a) satisfies (16) and begins to shift, whereas the robot in Fig. 7(c) does not satisfy (16) and does not begin to shift. Condition (16) cannot guarantee collision avoidance, but can reduce the risk of collision by setting the appropriate value as a_{nw}.

3) Shift of the connecting part: The connecting part can be shifted by moving the pitch angles $\psi_{i-1}, \psi_i,$ and ψ_{i+1} as shown in Fig. 7. Let the appropriate angle of the pitch joint against the step be $\alpha_d = \sin^{-1} \frac{h}{L}$, the start time of the shift be t_{st}, the end time of the shift be $t_{st} + t_\psi$, and let us define the desired values of pitch joints $\psi_{(i-1)d}, \psi_{id},$ and $\psi_{(i+1)d}$ as follows:

$$\psi_{(i-1)d} = -\alpha_d \left(1 - t'\right), \tag{17}$$

$$\psi_{id} = -\psi_{(i-1)d} - \sin^{-1}\left(\frac{h}{L} + \sin\psi_{(i-1)d}\right), \tag{18}$$

$$\psi_{(i+1)d} = -\psi_{(i-1)d} - \psi_{id}$$
$$= \sin^{-1}\left(\frac{h}{L} + \sin\psi_{(i-1)d}\right), \tag{19}$$

where t is the time, $t' = \frac{t - t_{st}}{t_\psi}$, and $t_{st} \leq t \leq t_{st} + t_\psi$. If the pitch joints satisfy (17), (18), and (19), the z length of the connecting part is h and the front and rear parts of the robot remain in contact with the ground.

The robot can ascend and descend higher steps by increasing the number of modules in the connecting part. We consider the case where the connecting part is the $i, \cdots, i + j - 1$-th module and the number of modules in the connecting part is $j > 1$. Fig. 12 shows an example of ascending a high step where the shape of the connecting part is straight and the robot shifts the connecting part in increments of one module. From Fig. 12(a) and (c), the robot must satisfy the following conditions to shift the connecting part:

[Condition 1] If $t' = 0$, $\psi_{i+j} = 0$.
[Condition 2] If $t' = 1$, $\psi_{i+j-1} = 0$.
[Condition 3] If $0 \leq t' \leq 1$, $\sum_{k=i-1}^{i+j-1} L \sin \Psi_k = -h$ and $\sum_{k=i-1}^{i+j} \psi_k = 0$.
The pitch angles $\psi_{i-1}, \cdots, \psi_{i+j-1}$ satisfying Conditions 1–3 are not unique and can be set as desired. However, these should not be set so as to cause a collision between the connecting part and the two planes during shifting. Fig. 12 shows an example of shifting on a high step.
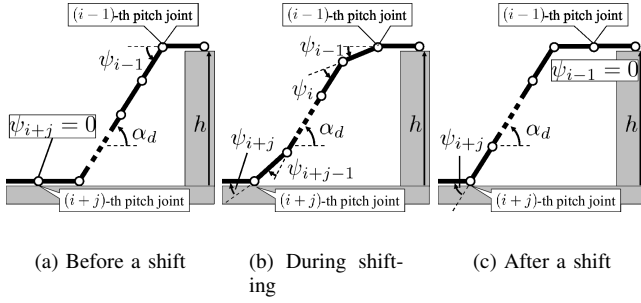
(a) Before a shift   (b) During shifting   (c) After a shift

Fig. 12. Shifting on a high step.

Fig. 13. The experimental system.

Fig. 14. Descending motion of the snake robot.

Fig. 15. Time responses of x_h, y_h, and θ_h in the descending experiment.

E. Dwell time of each mode

The mode changes in the following two cases.

I). The connecting part is shifted.

II). The grounded/ungrounded condition of the wheels changes depending on the environment.

In $\tilde{\boldsymbol{\phi}}_\sigma$, ϕ_i, which is the angle of the connecting part, and ϕ_{i+1}, which will become the angle of the connecting part at the next shift, are important because they need to converge to zero to satisfy assumption 1 and to start the shift. ϕ_i would previously have converged to zero when becoming the angle of the connecting part and there is no problem with its convergence. With respect to ϕ_{i+1}, the robot does not shift the connecting part until ϕ_{i+1} converges to zero because of shifting condition (14). Thus, the mode dwell time related to ϕ_{i+1} depends only on case II. In the descending case, if the robot moves forward, ϕ_{i+1} remains as one of the $\tilde{\boldsymbol{\phi}}_\sigma$ and the dwell time of the mode is sufficiently large. In the ascending case, it is not always true that the dwell time is sufficient. For example, if the forward velocity of the robot is significantly-fast or the convergence speed of ϕ_{i+1} is low, the dwell time is not enough, ϕ_{i+1} does not converge to zero, and the connecting part collides with the step because the robot cannot begin to shift the connecting part. These problems can be solved by reducing the forward speed or by increasing the convergence speed of ϕ_{i+1} (by increasing the corresponding feedback gain of the controller). In this paper, the dwell time of the mode related to ϕ_{i+1} is sufficiently large because we ensure that the corresponding feedback gain of the controller and the convergence speed of ϕ_{i+1} are adequate.

The $\tilde{\boldsymbol{\phi}}_\sigma$, except ϕ_i and ϕ_{i+1}, are used to change the shape of the robot. The dwell time of the mode related to these angles depends on cases I and II, and there is no guarantee that the length of dwell time is enough. However, these angles are not used for any essential condition that the robot must satisfy, and they do not cause significant problems in the locomotion of the robot even if the dwell time is not sufficient. These angles are merely used to approximate as best as possible the desired value of dwell time.

IV. EXPERIMENTS

Experiments were performed to confirm the effectiveness of the proposed control method. The experimental system is shown in Fig. 13. The snake robot has active joints and passive wheels with $l_{f0} = l_{b0} = 0.088$ m and $n = 8$. The pitch and yaw joints use Dynamixel MX-64R and MX-106R (ROBOTIS) actuators. The real-time position and attitude of the robot were measured by OptiTrack (NaturalPoint, Inc.), which is optical motion capture and tracking software. The joint angles were measured by the absolute encoder in the Dynamixel MX-64R and MX-106R. A PC was used to calculate the input and control the actuators with the PC and
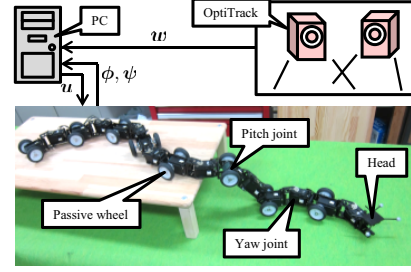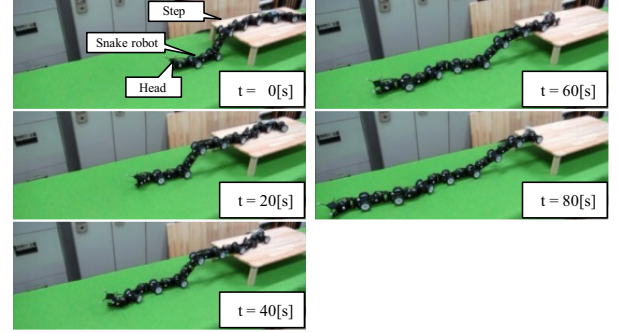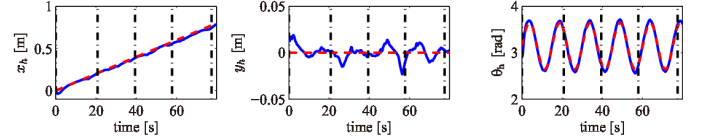
actuators connected in a daisy chain via an RS485 interface. We set the parameters of the controller to $\boldsymbol{K}_w = \text{diag}(0.5, 0.5, 1)$, $\boldsymbol{K}_\psi = 0.1\boldsymbol{I}_{n-1}$, $\boldsymbol{K}_{\tilde{\phi}_\sigma} = 0.5\boldsymbol{I}_{n_\sigma}$, $t_\psi = 5$ s, and $\epsilon = 0.05$.

A. Descent control

We set $h = -0.15$ m, $\boldsymbol{w}_d = [0.01t, \, 0, \, \pi + 0.5\sin(2\pi t/15)]^T$, and $x_{step} = -0.5$ m. Fig. 14 shows the motion of the robot in the descending experiment. Figs. 15 and 16 show the time responses of the controlled variables where the dashed line depicts the desired values. Figs. 17–19 show the time responses of ϕ_i, $\dot{\phi}_i$, and $\dot{\psi}_i$, respectively. In these figures, the vertical dot-dash lines depict the start time of each shift ($t = 0, 20.8, 39.4, 57.8, 77.4$).

Figs. 14–16 show that the connecting part of the robot shifts backwards sequentially without colliding with the step and that the controlled variable converges to the desired state. At $t \geq 10$, by which time the influence of the initial error has been sufficiently reduced, the maximum error values of x_h, y_h, and θ_h are 0.036 m, 0.017 m, and 0.084 rad, respectively. The tracking performance is acceptable because the values are sufficiently small.

As shown in Fig. 17, there are periods when the values of ϕ_3–ϕ_7 converge to zero. ϕ_3 is zero from the start of the experiment to $t = 20.1$ s at which time the connecting part shifts backwards because ϕ_3 is the connecting part at the start. ϕ_4–ϕ_7 become SCPs when the wheel of the corresponding module leaves the ground, and converge to zero, which is the desired value. As shown in Figs. 16 and 17, the connecting part shifts backwards after the corresponding SCP converges almost to zero. In Fig. 17, the intervals are shaded yellow if the corresponding joint belongs to the connecting part. The maximum values of $|\phi_3|$–$|\phi_7|$ during these intervals are 0.0092,
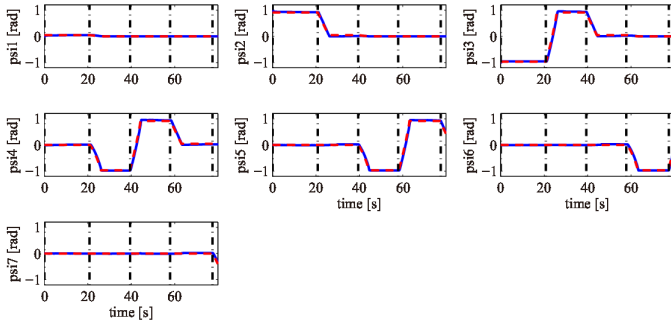
Fig. 16. Time responses of ψ_i in the descending experiment.
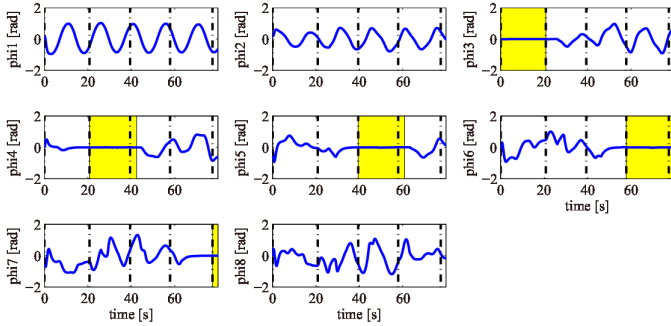
Fig. 17. Time responses of ϕ_i in the descending experiment.
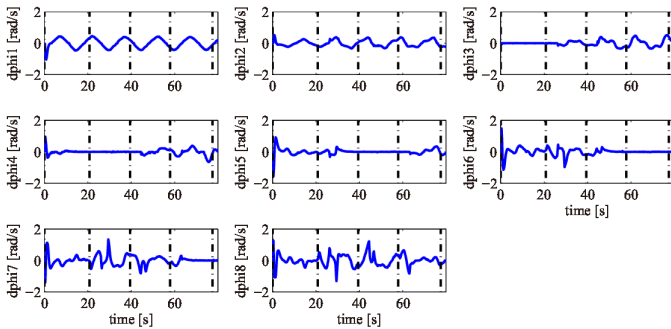
Fig. 18. Time responses of $\dot{\phi}_i$ in the descending experiment.
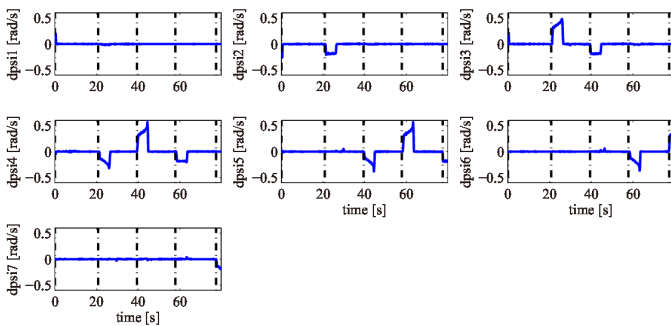
Fig. 19. Time responses of $\dot{\psi}_i$ in the descending experiment.

0.0092, 0.011, 0.015, and 0.0077 rad, respectively. We find that the values are sufficiently small, and thus assumption 1 is satisfied. The attitude of the connecting part is consistently normal to the step in Fig. 14. This is because the wheel of the connecting part is lifted by active lifting and the absolute angle of the connecting part is controlled by using the additional SCP.

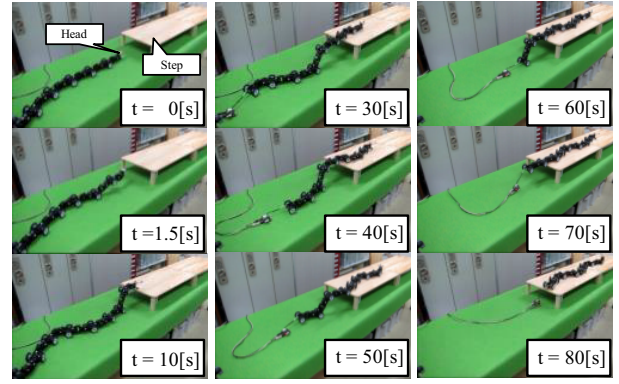Input of the yaw angles, $\dot{\phi}_i$ changes discretely owing to the switch

Fig. 20. Ascending motion of the snake robot.

in the mode of the robot caused by the shift and environment as shown in Fig. 18. For example, $\dot{\phi}_5$–$\dot{\phi}_8$ change discretely at $t = 25.8$ s at which time ψ_2–ψ_4 completes the change and the mode switches.

B. Whole transition of ascent control

We consider the whole transition between two planes for ascent control as shown in Fig. 3(a)–(d). First, we consider the motion lifting the robot's head from Fig. 3(a) to (b). This is likely to cause the yaw joint angle corresponding to the connecting part to be set to zero while lifting the head because the robot shifts the connecting part after the motion to lift the head. Thus, we set the second module as the connecting part and define the desired value of the pitch angles around the connecting part ψ_{1d}, ψ_{2d} as $\psi_{1d} = -\alpha_d t'$, $\psi_{2d} = \alpha_d t'$. This enables the robot to lift its head to the height of the front plane and to prepare to shift the connecting part later. Moreover, we add the condition $x_h > x_{step}$, which means that the head must reach the edge of the front plane before the first shift is started. Without this condition, the number of modules lifted increases and the pitch joint cannot hold the lifted modules because of the torque limit.

We set $h = 0.15$ m, $\boldsymbol{w}_d = [0.02t,\ 0,\ \pi + 0.6\sin(2\pi t/15)]^T$, $x_{step} = 0.2$ m, $t_\psi = 3$ s, and $a_{nw} = 2$. Fig. 20 shows the motion of the robot during the whole transition of the ascent. Figs. 21–22 show the responses of the robot similar to those discussed for the descending experiment. Figs. 20–22 show that the robot lifts up its head to the height of the front plane at $t \leq 3$, the connecting part of the robot shifts backwards sequentially without colliding with the step after the robot's head has reached the edge of the step ($x_h > x_{step}$), and the robot accomplishes the whole transition from the rear plane to the front plane. Fig. 21 shows that the controlled variable converges to the desired state with the maximum error values of x_h, y_h, and θ_h being 0.045 m, 0.022 m, and 0.089 rad, respectively.

As outlined above, the experimental results demonstrate the effectiveness of the control method. Note that the robot can climb and descend a higher step by increasing the number of links in the connecting part.

V. CONCLUSION

In this paper we proposed a control method to realize trajectory tracking of a robot's head and ascending and descending locomotion in a step environment consisting of two parallel planes. We focused on locomotion with shifting between two planes and introduced an assumption related to the connecting part and yaw angle to simplify the model and controller. We decomposed three-dimensional motion into motion parallel to the xy-plane and that parallel to the z-axis. In addition, we derived a model of the robot as a hybrid
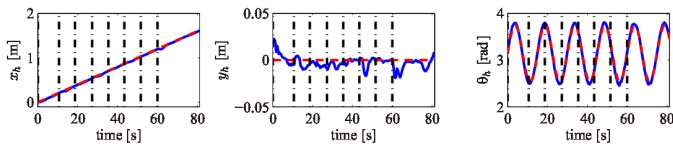
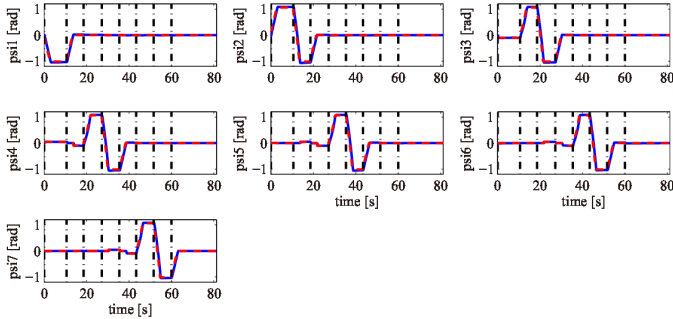Fig. 21. Time responses of x_h, y_h, and θ_h in the ascending experiment.

Fig. 22. Time responses of ψ_i in the ascending experiment.

system with switching on the xy-plane. We also proposed a controller consisting of a tracking controller and pitch reference generator based on the shifting method for the connecting part and active lifting to control the shape of the robot. Experimental results demonstrated the effectiveness of the proposed control method.

An advantage of the proposed method is that the method can accomplish trajectory tracking of a robot's head and ascending and descending a step without collision. Moreover, it can be implemented using a microcomputer and contributes to downsizing the robot because the computational overhead is smaller than that of a controller based on a dynamic model. However, a limitation of the method is that it is a kinematic controller, which assumes that the wheels do not slip sideways. It is not suitable if the dynamic effect of the motion of the robot is large or in the case of a slippery floor owing to the increased model error. Moreover, the steps considered in this research are the simplest in discrete three-dimensional environments, and the controller cannot be applied to non-parallel planes. Furthermore, it is necessary to observe the position and attitude of both the robot and step when using the proposed controller. These are the limitations of the proposed method. In future studies, we intend considering a control method for ascending and descending stairs in a more complicated environment, incorporating environmental recognition using only internal sensors, and modeling and control without velocity constraints, e.g., based on dynamics considering anisotropic friction.

REFERENCES

[1] S. Hirose, Biologically Inspired Robots (Snake-like Locomotor and Manipulator), Oxford University Press, 1987.
[2] S. Hirose S and A. Morishima, "Design and Control of a Mobile Robot With an Articulated Body," *Int. J. Robotics Research*, vol.9, no.2, pp.99-113, 1990.
[3] S. Hirose, E. F. Fukushima, and S. Tsukagoshi, "Basic Steering Control Methods for The Articulated Body Mobile Robot," *IEEE Control Systems Magazine*, vol.15, no.1, pp.5-14, 1995.
[4] K. L. Paap, F. Kirchner, and B. Klaassen, "Motion Control Scheme for a Snake-Like Robot," *Proc. IEEE Int. Symp. on Computational Intelligence in Robotics and Automation*, pp.59-63, 1999.
[5] A. A. Fjerdingen, P. Liljebäck, and A. A. Transeth, " A snake-like robot for internal inspection of complex pipe structures (PIKo)," *Proc. IEEE/RSJ Int. Conf. on Intelligent Robots and Systems*, pp.5665-5671, 2009.
[6] G. S. Chirikjian and J. W. Burdick, "The kinematics of hyper-redundant robot locomotion," *IEEE Trans. on Robotics and Automation*, vol. 11, pp.781–793, 1995.
[7] H. Yamada and S. Hirose, "Study on the 3D Shape of Active Cord Mechanism," *Proc. IEEE Int. Conf. on Robotics and Automation*, pp. 2890-2895, 2006.
[8] K. Lipkin, I. Brown, A. Peck, H. Choset, J. Rembisz, P. Gianfortoni, and A. Naaktgeboren, "Differentiable and piecewise differentiable gaits for snake robots," *Proc. IEEE/RSJ Int. Conf. on Intelligent Robots and Systems*, pp. 1864-1869, 2007.
[9] T. Kamegawa, T. Baba and A. Gofuku, "V-shift control for snake robot moving the inside of a pipe with helical rolling motion," *Proc. IEEE Int. Symp. on Safety, Security and Rescue Robotics*, pp.1-6, 2011.
[10] R. L. Hatton and H. Choset, "Generating gaits for snake robots: annealed chain fitting and keyframe wave extraction," *Autonomous Robots*, vol. 28-3, pp. 271-281, 2010.
[11] P. Liljebäck, K. Y. Pettersen, Ø. Stavdahl, and J. T. Gravdahl, "Controllability and Stability Analysis of Planar Snake Robot Locomotion," *IEEE Trans. on Aut. Cont.*, vol.56, no.6, pp.1365–1380, 2011.
[12] P. Liljebäck, I. U. Haugstuen and K. Y. Pettersen, "Path Following Control of Planar Snake Robots Using a Cascaded Approach," *IEEE Trans. on Cont. Sys. Tech*, vol.20, no.1, pp.111-126, 2012.
[13] P. Prautsch, T. Mita and T. Iwasaki, "Analysis and Control of a Gait of Snake Robot", *Trans. of IEEJ*, vol.120-D, pp.372-381, 2000.
[14] H. Date, Y. Hoshi and M. Sampei,"Locomotion Control of a Snake-Like Robot based on Dynamic Manipulability", *Proc. IEEE Int. Conf. on Intelligent Robots and Systems*, pp.2236-2241, 2001.
[15] M. Yamakita, M. Hashimoto and T. Yamada, "Control of Locomotion and Head Configuration for 3D Snake Robot", *Proc. IEEE Int. Conf. Robotics and Automation*, vol. 2, pp. 2055-2060, 2003.
[16] F. Matsuno and K. Mogi, "Redundancy Controllable System and Control of Snake Robot with Redundancy based on Kinematic Model", *Proc. IEEE Conf. on Decision and Control*, pp. 4791-4796, 2000.
[17] F. Matsuno and H. Sato, "Trajectory tracking control of snake robot based on dynamic model," *Proc. IEEE Int. Conf. on Robotics and Automation*, pp. 3040-3046, 2005.
[18] M. Tanaka and F. Matsuno, "Modeling and Control of Head Raising Snake Robots by Using Kinematic Redundancy," *J. of Intelligent and Robotic Systems*, vol.75, no.1, pp.53-69, 2014.
[19] M. Tanaka, F. Matsuno, "Control of Snake Robots with Switching Constraints: trajectory tracking with moving obstacle," *Advanced Robotics*, vol.28, issue 6, pp.415-429, 2014.
[20] T. Kamegawa, T. Yamasaki, H. Igarashi and F. Matsuno, "Development of The Snake-like Rescue Robot'KOHGA'," *IEEE Int. Conf. on Robotics and Automation*, pp. 5081-5086, 2004.
[21] H. Fukushima, S. Satomura, T. Kawai, M. Tanaka and F. Matsuno, "Modeling and Control of a Snake-like Robot Using the Screw Drive Mechanism," *IEEE Trans. on Robotics*, vol.28, no.3, pp.541-554, 2012.
[22] H. Tsukano, M. Tanaka and F. Matsuno, "Control of a Snake Robot on a Cylindrical Surface Based on a Kinematic Model," *9th IFAC Symposium on Robot Control*, pp.865-870, 2009.
[23] G. Granosik, "Hypermobile Robots –the Survey," *J. of Intelligent and Robotic Systems*, vol.75, no.1, pp.147–169, 2014.
[24] K. -U. Scholl, V. Kepplin, K. Berns, and R. Dillmann, "Controlling a Multijoint Robot for Autonomous Sewer Inspection," *Prc. IEEE Int. Conf. on Robotics and Automation*, pp.1701-1706, 2000.
[25] H. Yamada and S. Hirose, "Development of Practical 3-Dimensional Active Cord Mechanism ACM-R4," *J. of Robotics and Mechatronics*, vol.18, no.3, pp.305-311, 2006.
[26] H. Yamada, S. Takaoka, and S. Hirose, "A snake-like robot for real-world inspection applications (the design and control of a practical active cord mechanism)," *Advanced Robotics*, vol.27, no.1, pp.47-60, 2013.
[27] K. Kouno, H. Yamada, and S. Hirose, "Development of Active-Joint Active-Wheel High Traversability Snake-Like Robot ACM-R4.2," *J. of Robotics and Mechatronics*, vol.25, no.3, pp.559-566, 2013.
[28] B. Murugendran, A. A. Transeth, and S. A. Fjerdingen, "Modeling and Path-following for a Snake Robot with Active Wheels," *IEEE/RSJ Int. Conf. on Intelligent Robots and Systems*, pp.3643-3649, 2009.
[29] A. S. Morse, "Supervisory Control of Families of Linear Set-Point Controllers–Part 1: Exact Matching," *IEEE Trans. on Automatic Control*, vol. 41, no. 10, pp. 1413-1431, 1996.
[30] D. Liberzon, *Switching in Systems and Control*, Birkhauser, 2003.